Infrasound from large surf

M. Garcés,[1] J. Aucan,[1] D. Fee,[1] P. Caron,[1] M. Merrifield,[1] R. Gibson,[2] J. Bhattacharyya,[2] and S. Shah[2]

Received 28 October 2005; revised 6 December 2005; accepted 21 December 2005; published 10 March 2006.

[1] Simultaneous infrasonic, visual, and ocean-bottom pressure sensor observations of large swells on the island of Kauai and small to medium-sized surf on the island of Hawaii yielded a clear relationship between breaking wave height and low-frequency atmospheric sound amplitudes in the 1–20 Hz frequency range. These experiments confirmed that infrasound can be generated by barreling waves as well as by waves crashing against rocky shorelines and exposed ledges. As will be demonstrated in a companion paper, breaking wave period may also be extracted from infrasound data. The results of these experiments demonstrate that low-frequency sound may be used for real-time estimates of the amplitude, period, and spatial distribution of surf in the littoral zone, with a potential application to the identification of breaking wave types.
Citation: Garcés, M., J. Aucan, D. Fee, P. Caron, M. Merrifield, R. Gibson, J. Bhattacharyya, and S. Shah (2006), Infrasound from large surf, *Geophys. Res. Lett.*, *33*, L05611, doi:10.1029/2005GL025085.

1. Introduction

[2] Infrasonic stations located near ocean shores routinely record infrasound from breaking waves. *Garcés et al.* [2003] recognized a clear relationship between infrasonic amplitude in the 1–5 Hz range and breaker height, and postulated that a breaking wave may generate infrasound by barreling (plunging), slamming against a cliff, or by impacting against dry reef. *Le Pichon et al.* [2004] corroborated the relationship between infrasonic and ocean wave amplitudes and located active surf regions along the coastline of Tahiti. *Arrowsmith and Hedlin* [2005] reported surf infrasound propagating over 200 km inland under favorable wind and swell conditions.

[3] This paper presents the initial results of two experiments designed to further our understanding of surf infrasound sources and to help develop new methods for remote, real-time assessment of littoral sea state. Two diverse coastal environments were selected at opposite ends of the Hawaiian chain. The shoreline at Makalawena beach, Hawaii (Figure 1), consists primarily of old lava flows, whereas the shoreline at Polihale beach, Kauai, is all sand. During the experiments, the swell height at Makalawena did not exceed 1.5 m, whereas at Polihale the swell height reached 7 m. Since the breaker height is approximately twice the open sea swell height, the large plunging waves (>40′ faces) observed at Polihale during the experiment triggered a high swell warning through the Hawaiian chain.

2. Instrumentation and Signal Processing

[4] The portable data acquisition system we used to collect near-shore infrasound data is similar to that used by *Garcés et al.* [2003], except that superior Chaparral 2 and Chaparral 5 sensors were deployed. The frequency response of both sensor types is flat within the passband of interest (0.1–50 Hz), with a nominal sensitivity of ~100 mV/Pa. We used 4-element triangular arrays with a central element and an aperture of ~100 m at Makalawena and ~60 m at Polihale (Figure 1). Surface wind speed and direction were also recorded near the central array element. Tree cover at the array sites provided the first level of wind shelter, high cliffs provided additional wind cover at Polihale, and porous hoses were used at the microphones for wind noise reduction. All data channels were recorded by Geotech DL-24 digitizers at 40 samples per second (sps) at Makalawena and 100 sps at Polihale. GPS timing and UTC are used for all infrasound data.

[5] Sea-Bird SBE26 pressure gauges, sampled at 1 sps, were deployed at both experimental sites. These gauges were emplaced on the sea bottom via kayak at Makalawena and by divers at Polihale, and provided a measure of the sea level and wave height above the instruments (Figure 1). The timing accuracy of the ocean bottom sensors is ~1 s. One video camera was deployed at various locations for filming during optimal lighting and swell conditions, and the timing accuracy of the camera is also ~1 s. An infrared camera was also operated for part of the Makalawena experiment. Fortunately, ocean waves propagate slowly compared to sound and light, so for near-field observations it is possible to identify sound and visual signals associated with wave-breaking events.

[6] Three ocean bottom pressure gauges and two infrasound arrays with similar geometry were deployed ~1 km apart from each other at Makalawena beach during January 3–14, 2005 (only one of the configurations of infrasonic sensors and pressure gauges is shown in Figure 1). Three pressure gauges, roughly aligned perpendicular to the coastline, and one infrasound array were deployed at Polihale during March 4–12, 2005. The squares in Figure 1 denote the video camera locations used in the analysis.

[7] We applied the PMCC algorithm of *Cansi* [1995] to detect coherent infrasonic energy across the array and extract the speed, arrival angle, and amplitude of the detected arrivals. The azimuth estimates were used to correlate the acoustic and visual signals. The ocean bottom sensor data was processed using standard algorithms to extract the significant wave height (average of the highest one-third of the swells) and dominant period of the swells,

[1]Department of Oceanography, School of Ocean and Earth Science and Technology (SOEST), University of Hawaii at Manoa, Honolulu, Hawaii, USA.
[2]BBN Technologies, Arlington, Virginia, USA.

0094-8276/06/2005GL025085

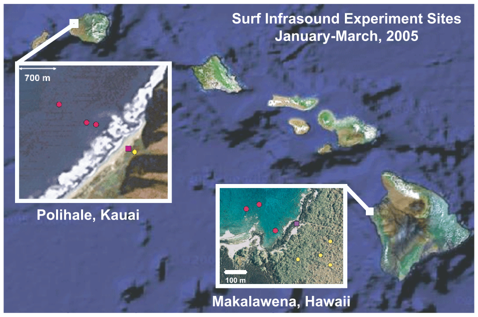

Figure 1. Experimental sites in Hawaii and Kauai for the surf infrasound experiments performed in the high surf season of winter 2004–2005. Both sites have a northwest exposure, but Polihale is completely exposed while the island chain partially blocks NW swells approaching Makalawena [*Garcés et al.*, 2003]. The red circles denote ocean bottom pressure sensors, the purple squares video camera locations, and the yellow circles the infrasonic sites. The Makalawena map shows individual microphone locations for one of the two arrays, whereas the yellow circle in the Polihale map denotes the approximate aperture of a four-element array.

which were compared to the infrasonic amplitudes and spectra.

3. From Small to Large Waves

[8] As discussed by *Garcés et al.* [2003], the west coast of Hawaii is routinely deprived of northwest swells by obstruction from the island chain. Makalawena beach was selected for its remarkable ability to receive the north and northeast swells typical of the early and late winter season. However, no large or significant swells from the targeted directions were recorded during the experiment, although even the smallest days produced numerous coherent infrasonic signals. The highest significant wave height recorded during the Makalawena experiment was ~1.5 m, which produced a variety of infrasonic arrivals from all possible ocean azimuths. We realized that an irregular rocky coastline with multiple potential breaking zones and depths produces non-unique source solutions that are very difficult to interpret. Synchronous detections from the two infrasound arrays at Makalawena beach rarely resulted in consistent back-azimuths, and when they did it was not clear what part of the coast or bathymetry produced the signal. Simultaneous analysis of infrasound array data and video images during days of small surf on the bay shown in Figure 1 yielded convincing evidence that waves plunging against shallow lava shelves and rocks produced infrasound. During these days of small surf, no waves broke in the relatively deep center of the bay and all infrasound arrivals from those azimuths were produced right at the lava shore. In addition to confirming the generation of infrasound by impact of water against solids and the proportionality of acoustic amplitude to wave height, we also learned that the bandwidth of interest for surf infrasound extended beyond 15 Hz. Thus we planned the next experiment in a simpler coastal environment, with a smaller array designed for optimal reception at higher infrasonic frequencies.

[9] Polihale beach is completely exposed to any swell with a northwesterly component. During March 4–12, 2005, the swell height never dropped below 1 m (overhead breakers), and reached heights of 7 m. Although plunging breakers were dominant, surging and spilling breakers were also observed, as well as substantial backwash and variable rip tides, depending on the winds, swell height and tides. However, except for the nearest waves slamming against the water-saturated sand, wave breaking processes at Polihale involved either water-water or water-air interactions, thereby simplifying the interpretation of the observed signals.

[10] A comparison of the amplitude and spectral content of one ocean bottom pressure sensor, one microphone, and the wind speed at Polihale is shown in Figure 2. The pressure gauge and microphone records shown are representative of signals from the other sensor elements.

[11] Figure 2a shows the significant wave height, in meters, and Figure 2b the ocean wave spectra computed for 1 hr windows. The large swells of March 6 (5 m) and March 8 (7 m) can be recognized by their long periods, large amplitudes, and multiple frequency bands in the ocean wave data. Figure 2c shows the hourly root mean squared (rms) infrasonic amplitude within the 2–5 Hz band, and Figures 2d and 2e show the infrasonic spectrogram within the 1–20 Hz and the 0.4–1 Hz bands, respectively. The rms infrasonic amplitude and spectrogram within the 1–20 Hz band match well the significant wave height and the swell spectrogram. Although there appears to be substantial energy from surf in the 0.4–1 Hz band, it cannot always be separated from background noise induced by high winds (Figure 2f). This observation is site-dependent, as an array that is not protected from wind by natural barriers or forest cover would be affected by wind noise at all frequency bands.

[12] Microbaroms [e.g., *Willis et al.*, 2004] and their seismic counterparts, microseisms [e.g., *Bromirski et al.*, 2005], are well known, persistent signals attributed to the nonlinear interaction of ocean swells in the open seas or near coastlines. The spectrogram in the microbarom band of 0.1–0.4 Hz (Figure 2g) shows the spectral peak bifurcation associated with large swells [*Garcés et al.*, 2004] preceding the arrival of the March 6 swell, and tapering down to the more typical microbarom signature with a dominant spectral peak. The noise contribution from high winds, and the weather perturbations that accompany them, can be observed as intense broadband features also observed in the 0.4–1 Hz acoustic band.

[13] The primary conclusions drawn from Figure 2 are that (1) the source bandwidth of infrasound signals from surf may extend from 0.4–20 Hz, with the observable lower frequencies limited by more energetic ambient noise sources, and (2) the infrasonic rms amplitude is related to the significant wave height. Therefore a single microphone, properly located in a low-wind environment near the shore, is capable of providing an estimate of local wave height. As will be shown in a separate paper, it is also possible to estimate the breaking wave period from the acoustic data, thereby extending the usefulness of the acoustic recordings.

[14] We also computed rms infrasonic amplitudes in 2 Hz frequency bands, and compared them to the

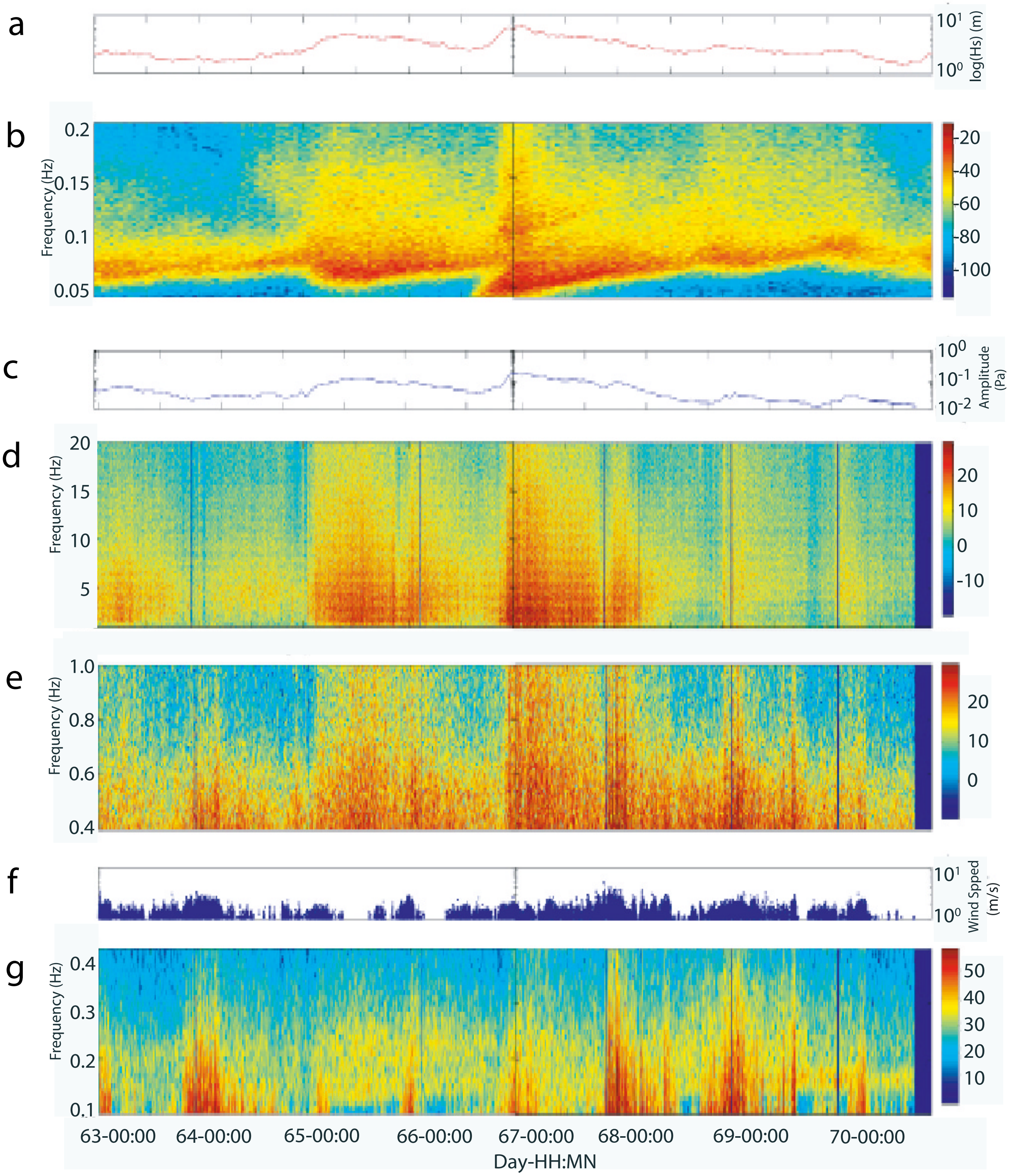

Figure 2. Comparison of the amplitude and spectral content of ocean bottom pressure sensor, microphone, and wind sensor observations at Polihale. Dates are in Julian day, with day 63 as March 4, 2005. (a) Significant wave height, in meters, (b) ocean wave height spectrogram, expressed in dB, (c) hourly rms infrasonic amplitude, in Pa, in the 2–5 Hz band, (d) infrasonic spectrogram, with logarithmic color scale, in the 1–20 Hz band, (e) infrasonic spectrogram, with logarithmic color scale, in the 0.4–1 Hz band, (f) wind speed, in m/s, and (g) infrasonic spectrogram, with logarithmic color scale, in the microbarom band of 0.1–0.4 Hz. Two broad microbarom peaks can be observed before March 10 (day 69), and a single dominant peak thereafter.

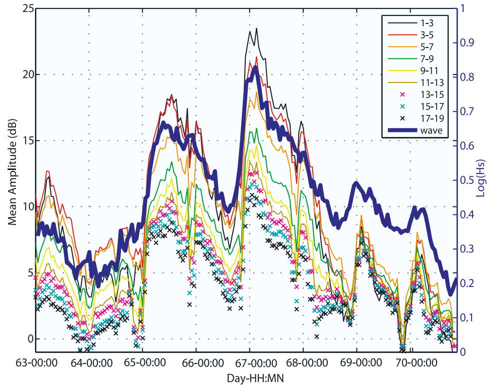

Figure 3. Comparison of significant wave height, in meters (solid blue line), and infrasonic amplitude, expressed in dB re 20 μPa, in 2 Hz frequency bands.

significant wave height (Figure 3). Although the trends in all acoustic bands follow the wave height, the details sometimes differ. The two large swells starting on March 6 and March 8, respectively, are clearly seen in all acoustic bands, but some of the smaller swell days produced more infrasound than others. The differences between the wave height and acoustic observations may be because the microphones measure the sound produced by the wave breaking dynamics, which are affected by swell direction, tide, wind, and littoral circulation patterns, whereas the ocean bottom pressure sensors measure the ocean swell arriving from all directions. Preliminary analyses indicate that correlations between rms infrasonic amplitude and wave height are highest in the ∼5–15 Hz frequency band. Details of the optimal correlation parameters vary depending on sensor locations and possibly wave breaking types. Our preliminary studies suggest that the optimal infrasonic frequency band for surf monitoring may be determined by the coastal environment.

4. Concluding Remarks

[15] Our initial results suggest that low-frequency sound can be used to monitor the energetics, spatial distribution, and temporal variability of different types of breaking ocean waves. The two experiments that were performed in very different coastal environments confirmed that infrasound may be produced by plunging waves as well as by surf impinging against cliffs and exposed reefs. These data will be used in conjunction with other ongoing experiments to characterize and identify different source processes. During high surf, most of the surf infrasound energy appears to be in the 0.4–20 Hz frequency band, with the lower frequencies being affected by large-scale turbulence from wind. Preliminary analyses in this and the companion paper of *Aucan et al.* [2006] demonstrate that it is possible to extract the height and period of breaking waves from single-sensor infrasound data. The directional discrimination capabilities of infrasound arrays, perhaps coupled with intelligent waveform recognition and classification algorithms, may also permit the identification of distinct regions of wave action and the recognition of different wave breaking types in the surf zone.

[16] **Acknowledgments.** This work was funded by the National Defense Center of Excellence for Research in Ocean Sciences (CEROS). CEROS is funded by the Defense Advanced Research Projects Agency (DARPA) through grants to and agreements with the Natural Energy Laboratory of Hawaii Authority (NELHA), an agency of the Department of Business, Economic Development and Tourism, State of Hawaii. This report does not necessarily reflect the position or policy of the Government, and no official endorsement should be inferred. Many thanks to A. Le Pichon and an anonymous reviewer for their thoughtful recommendations.

References

Arrowsmith, S. J., and M. A. H. Hedlin (2005), Observations of infrasound from surf in southern California, *Geophys. Res. Lett.*, *32*, L09810, doi:10.1029/2005GL022761.

Aucan, J., D. Fee, and M. Garcés (2006), Infrasonic estimation of surf period, *Geophys. Res. Lett.*, *33*, L05612, doi:10.1029/2005GL025086.

Bromirski, P., F. Duennebier, and R. Stephen (2005), Mid-ocean microseisms, *Geochem. Geophys. Geosyst.*, *6*, Q04009, doi:10.1029/2004GC000768.

Cansi, Y. (1995), An automatic seismic event processing for detection and location: The P.M.C.C. method, *Geophys. Res. Lett.*, *22*, 1021–1024.

Garcés, M., C. Hetzer, M. Merrifield, and J. Aucan (2003), Observations of surf infrasound in Hawai'i, *Geophys. Res. Lett.*, *30*(24), 2264, doi:10.1029/2003GL018614.

Garcés, M., M. Willis, C. Hetzer, A. Le Pichon, and D. Drob (2004), On using ocean swells for continuous infrasonic measurements of winds and temperature in the lower, middle, and upper atmosphere, *Geophys. Res. Lett.*, *31*, L19304, doi:10.1029/2004GL020696.

Le Pichon, A., V. Maurer, D. Raymond, and O. Hyvernaud (2004), Infrasound from ocean swells observed in Tahiti, *Geophys. Res. Lett.*, *31*, L19103, doi:10.1029/2004GL020676.

Willis, M., M. Garcés, C. Hetzer, and S. Businger (2004), Infrasonic observations of open ocean swells in the Pacific: Deciphering the song of the sea, *Geophys. Res. Lett.*, *31*, L19303, doi:10.1029/2004GL020684.

J. Aucan, P. Caron, D. Fee, M. Garcés, and M. Merrifield, Department of Oceanography, School of Ocean and Earth Science and Technology (SOEST), University of Hawaii at Manoa, 1000 Pope Road, Honolulu, HI 96822, USA. (milton@isla.hawaii.edu)

J. Bhattacharyya, R. Gibson, and S. Shah, BBN Technologies, 1300 North 17th Street, Suite 400, Arlington, VA 22209, USA.